Journal of Photochemistry and Photobiology B: Biology 140 (2014) 228–239

Contents lists available at ScienceDirect

Journal of Photochemistry and Photobiology B: Biology

journal homepage: www.elsevier.com/locate/jphotobiol

Unveiling Zn hyperaccumulation in *Juncus acutus*: Implications on the electronic energy fluxes and on oxidative stress with emphasis on non-functional Zn-chlorophylls

D. Santos, B. Duarte *, I. Caçador

Centre of Oceanography of the Faculty of Sciences of the University of Lisbon (CO), Campo Grande, 1749-016 Lisbon, Portugal

ARTICLE INFO

Article history:
Received 22 April 2014
Received in revised form 30 June 2014
Accepted 29 July 2014
Available online 19 August 2014

Keywords:
Hyperaccumulator
Zinc-chlorophylls
Photochemistry
Electronic transport
Oxidative stress

ABSTRACT

Juncus acutus arises as possible hyperaccumulator specie, tolerating exogenous Zn concentrations as high as 60 mM. Zinc concentrations here detected in seedlings germinated in the presence high Zn concentrations, were above the described upper toxic levels for higher plants. Even at the highest Zn concentration, growth inhibition only accounted to approximately 30% of control seedlings biomass, presenting an EC_{50} value in the range of 10–20 mM of metal. PSII quantum yields showed a marked decline, reflection of changes in the thylakoid structure on the PSII electron donor sites. In fact, the electron transport rate was severely affected by Zn in seedlings exposed to higher Zn concentrations leading to a decrease in their maximum electronic transport rate and consequently presenting lower light saturation and lower photosynthetic efficiencies. Although light absorption capacity was not affected by Zn exposure and uptake, energy trapping flux in the photosynthetic apparatus and transport throughout the electronic chain was severely impaired. This lack of efficiency is related with non-functional Zn-chlorophylls formation. There was a strong linear correlation between exogenous Zn concentration applied and the concentration actually verified in the seedlings tissue with the concentration of both ZnChl a and b. There was also a gradual loss of connectivity between the antennae of the PSII units being this more evident at the higher Zn concentrations and thus impairing the energetic transport. The reduction in light harvesting efficiency, leads inevitably to the accumulation of redox energy inside the cells. To counteract ROS generation, all anti-oxidant enzymatic activities (except catalase) showed a proportional response to exogenous and *in vivo* Zn concentrations. Not only this plant appears to be highly tolerant to high Zn concentrations, but also it can overcome efficiently the damage produced during this uptake by efficiently dissipating the excessive cellular redox potential accumulated, essentially due to Zn incorporation into the chlorophyll molecule.

1. Introduction

Salt marsh ecosystems, are of great ecological importance. *Sarcocornia perennis*, *Sacocornia fruticosa*, *Spartina maritima*, *Halimione portulacoides* [5] and *Juncus acutus* [31,4] are some of the halophyte species commonly inhabitant in this environments, in Mediterranean marshes. Due to their location near or alongside estuaries, these ecosystems are often exposed to high anthropogenic pressures and considered as natural sink of heavy metals from industrial and urban sewage [38,5]. Despite the fact that some halophyte species from salt marshes can withstand some degree of contamination, excessive concentration of metals in the soil, driven from long-term accumulation or toxic discharges, can not only cause damages in the plants, but also be potentially harmful to human health, through food chain.

Metals like zinc (Zn), iron (Fe) and nickel (Ni) are essential to plant metabolism at lower concentrations, however in higher concentrations can cause disorders. Zinc (Zn), as other essential metals like copper (Cu), can become toxic to plants whenever their concentrations are above their nutritional threshold [29]. At organismal level, excess Zn inhibits seed germination, plant growth [36] root development [26] and causes leaf chlorosis [16]. At cellular level, excess Zn can significantly alter mitotic activity [45], affect membrane integrity and permeability [48] and even induce cell death [7]. Excessive Zn concentrations can also cause imbalances between production and scavenging of reactive oxygen species, inducing oxidative stress conditions. To counteract the effect of free radicals, plants developed a battery of defences that includes

* Corresponding author. Tel.: +351 217 500 009.
E-mail address: baduarte@fc.ul.pt (B. Duarte).

http://dx.doi.org/10.1016/j.jphotobiol.2014.07.019
1011-1344/

some antioxidant enzymes like superoxide dismutase (SOD), catalase (CAT), guaiacol peroxidise (GPx) and ascorbate peroxidise (APx). These enzymes have a fundamental role in the O_2 and H_2O_2 production by ROS catalysis. These oxygen forms are far less harmful to the organism and can result for example from the dismutation of superoxide ion (O^{2-}), preventing serious cellular damage. Previous works have shown that excess Zn induces oxidative stress and lipid peroxidation [43,27]. Several recent studies [27,9,8,56,52] have demonstrated the effects of Zn stress on the activity of many antioxidative enzymes (APx, SOD, POD and CAT) and antioxidant contents (ascorbate and GSH) in plants.

Nevertheless, ROS generation is a rather transversal effect from almost all excessive cations in cellular compartments. In fact, Zn has another a potentially more damaging effect in plant bioenergetics, by substituting the Mg atom at the chlorophyll reaction center. Hence, the formation of minor proportions of [Zn]-Chl relative to the total Chl may already inhibit photosynthesis completely, affecting the overall cell bioenergetics and redox homeostasis [25]. This substitution effect is rather well known and was already described in algae [25] and in higher plants [37].

Juncus acutus Lam. (*J. acutus*) is highly common halophyte specie in Portuguese marshes, found in several kinds of sediments from sandy to muddy, gathering this way an increased colonization potential in all sorts of salt marshes [4]. Alongside, Zn is highly abundant in the Earth's crust and has a widespread role in industrial processes, with inevitable inputs to the surrounding environment, especially in estuarine systems [11]. Therefore, *J. acutus* widespread presence and wide range of habitat physical attributes, makes this halophyte ideal for testing the effects, that a highly abundant metal such as Zn, can have in the establishment of a halophytic specie independently the marsh type [4].

In the present work, the authors aimed to understand zinc effects in *J. acutus* seed germination, growth, photosynthetic apparatus as well as in photosynthetic pigments (including Zn substituted chlorophylls) and seedlings antioxidant response to acute metal stress, for use as potential biomarkers. This approach aims to unveil the Zn hyperaccumulation ability in this specie, understanding the effect of this specific metal on the seedling survival and its implications on cellular bioenergetics and redox homeostasis.

2. Materials and methods

2.1. Seed harvest and incubations

Juncus acutus seeds were harvested in November 2011 in an undisturbed salt marsh of Tagus estuary within the old World Exposition 98' site. All the collected flowers were brought to the laboratory and kept in dry conditions. Seeds were incubated in ¼ Hoagland solution supplemented with $ZnSO_4$ (Sigma–Aldrich Ultra-Pure) in order to make the desired concentrations (10, 20, 40 and 60 mM). Zinc treatments were established by supplementing ¼ Hoaglands solution with $ZnSO_4{\cdot}7H_2O$ to achieve the target concentrations comparable to previous studies with halophytes using acute heavy metal concentrations in salt marshes [6,32]. The control, 0 mM Zn treatment, had exactly 0.002 mM Zn, as Hoaglands solution contains a small amount of Zn as essential nutrient. Approximately 20 seeds were placed in each petri dish with a Whatman GF/C filter as solid substrate. Each treatment (n = 3 petri dish, approx. 60 seeds) was soaked with 800 μL of the correspondent Zn concentration solution. The petri dishes were sealed with Parafilm and placed in a FytoScope Chamber (Photon System Instruments, Czech Republic) in the dark at 25 °C. Every three days, germinated seeds were counted until a maximum of 15 days. After germination (approximately after 6 days of incubation), the petri dishes were placed in light conditions (150 μmol photons m^{-2} s^{-1}) in a 16 h/8 h day–night regime using a sin function to simulate sunrise–midday–sunset conditions. At the end of the experiment, seedlings were collected and used for analysis. All seedlings for biochemical analysis were flash-frozen in liquid-N_2. Seedlings were also weighted and measured for total length. The Germination Index (GI) and germination rates were calculated by the following formulas:

$$GR = \frac{\sum(\text{Number of germinated seed in n days} \times \text{number of days})}{\text{total number of days}}$$

$$GI = \sum \frac{\text{Number of germinated seeds}}{\text{Days since first count}}$$

2.2. Metal content analysis

Dry homogenized material was digested by adding 2 ml HNO_3/$HClO_4$ (7:1, v/v) in a Teflon reactor and heated at 110 °C for 6 h. After cooling overnight, the digestion products were filtered through Whatman No. 42 (2.5 μm of pore diameter) filters and diluted with distilled water to a total volume of 10 ml. Zinc concentrations in the extracts were determined by atomic absorption spectrometry (Perkin–Elmer A Analyst 100). International certified reference materials (CRM 145, CRM 146 and BCR 62) were used to ensure accuracy and precision of the extraction and analytical. The concentrations in the reference materials determined by FAAS were not statistically different from their certified ones (t student; a = 0.05).

2.3. PAM fluorometry

Modulated chlorophyll fluorescence measurements were made in attached leaves in field with a FluoroPen FP100 PAM (Photo System Instruments, Czech Republic). All the measurements in the dark-adapted state were made after darkening of the leaves for at least 30 min. The minimal fluorescence (F_0) in dark-adapted state was measured by the measuring modulated light, which was sufficiently low (<0.1 μmol m^{-2} s^{-1}) not to induce any significant variation in fluorescence. The maximal fluorescence level (F_M) in dark-adapted state was measured by a 0.8 s saturating pulse at 8000 μmol m^{-2} s^{-1}. The maximum photochemical efficiency was assessed as $(F_M - F_0)/F_M$. The same parameters were also measured in light-adapted leaves, being F'_0 the minimum fluorescence, F'_M the maximum fluorescence and the operational photochemical efficiency. Rapid light curves (RLC) measurements, in dark-adapted leaves, were attained using the pre-programed LC1 protocol of the FluoroPen, consisting in a sequence of pulses from 0 to 500 μmol m^{-2} s^{-1}. During this protocol the F_0 and F_M as well as the maximum photochemical efficiency were measured. Each Φ_{PSII} measurement was used to calculate the electron transport rate (ETR) through photosystem II using the following equation: $ETR = \Phi_{PSII} \times PAR \times 0.5$, where PAR is the actinic photosynthetically active radiation generated by the FluoroPen and 0.5 assumes that the photons absorbed are equally partitioned between PSII and PSI [18]. Without knowledge of the actual amount of light being absorbed, fluorescence measurements can only be used as an approximation for electron transport [1,2] and [46]. Rapid light curves (RLC) were generated from the calculated ETRs and the irradiances applied during the rapid light curve steps. Each RLC was fitted to a double exponential decay function in order to quantify the characteristic parameters, alpha and ETR_{max} [42]. The initial slope of the RLC (α) is a measure of the light harvesting efficiency of photosynthesis and the asymptote of the curve, the maximum rate of photosynthesis (ETR_{max}), is a measure of the capacity of the photosystems to utilize the absorbed light energy [30]. The onset of light

Table 1
Summary of fluorometric analysis parameters and their description.

Photosystem II efficiency	
F'_0 and F_0	Basal fluorescence under weak actinic light in light and dark adapted leaves
F'_M and F_M	Maximum fluorescence measured after a saturating pulse in light and dark adapted leaves
F'_v and F_v	Variable fluorescence light (F'_M–F'_0) and dark (F_M–F_0) adapted leaves
PSII operational and maximum quantum yield	Light and dark adapted quantum yield of primary photochemistry, equal to the efficiency by which an absorbed photon trapped by the PSII reaction center will result in reduction of Q_A to Q_A^-
Rapid light curves (RLCs)	
rETR	Relative electron transport rate at each light intensity (rETR = QY × PAR × 0.5)
α	Photosynthetic efficiency, obtained from the initial slope of the RLC
OJIP derived parameters	
ψ_{P0}	Maximum Yield of Primary Photochemistry
ψ_{E0}	Probability that an absorbed photon will move an electron into the ETC
ψ_{D0}	Quantum yield of the non-photochemical reactions
φ_0	Probability of a PSII trapped electron to be transported from Q_A to Q_B
Area	Area above the fluorescence Kautsky curve. Directly related to the size of the acceptor pool of the PSII, including quinones and plastoquinone
P_G	The grouping probability is a direct measure of the connectivity between the two PSII units (Strasser and Stribet, 2001)
Diving force for photosynthesis (DF ABS)	DF ABS = DF RC + DF ψ_{P0} + DFφ)
Driving force for trapping electronic energy (DF ψ_{P0})	DFψ_{P0} = log (ψ_{P0}/(1 − ψ_{P0}))
Driving force for electron transport (DFφ)	DFφ = log (φ_0/(1 − φ_0))
Driving force for energy absorption (DF RC)	DF RC = log(RC/ABS)

saturation (E_k) was calculated as the ratio between ETR_{max} and α Excitation light of 650 nm (peak wavelength) from array of three light and emitting diodes is focused on the surface of the leaf to provide a homogenous illumination. The light intensity reaching the leaf was 3000 μmol m^{-2} s^{-1}, which was sufficient to generate maximal fluorescence in all individuals. The fluorescence signal is received by the sensor head during recording and is digitized in the control unit using a fast digital converter. The OJIP transient depicts the rate of reduction kinetics of various components of PS II. When dark-adapted leaf is illuminated with the saturating light intensity of 3500 μmol m^{-2} s^{-1} it exhibits a polyphasic rise in fluorescence (OJIP). Each letter reflects distinct inflection in the induction curve. The level O represents all the open reaction centers at the onset of illumination with no reduction of Q_A (fluorescence intensity lasts for 10 as). The rise of transient from O to J indicates the net photochemical reduction of Q_A (the stable primary electron acceptor of PS II) to Q_A^- (lasts for 2 ms). The phase from J to I was due to all reduced states of closed RCs such as Q_A^- Q_B^-, Q_A Q_B^{2-} and Q_A^- Q_B H_2 (lasts for 2–30 ms). The level P (300 ms) coincides with maximum concentration of Q_A^- Q_B^2 with plastoquinol pool maximally reduced. The phase P also reflects a balance between light incident at the PS II side and the rate of utilization of the chemical (potential) energy and the rate of heat dissipation [57]. From this analysis several photochemical parameters were attained: Maximum Yield of Primary Photochemistry (Phi P_0), the probability that an absorbed photon will move an electron into the ETR (Phi E_0), the number of Q_A redox turnovers until F_M is reached (N), the number of electrons that flow from Q_A^- to the ETR (S_M) and the Performance Index [22]. From this analysis several photochemical parameters were attained (Table 1).

2.4. Gauss peak spectra pigment analysis

Seeds for pigment analysis were freeze-dried in the dark during 48 h, after which they were grinded in pure acetone with a glass rod. To ensure complete disaggregation of the seed material, samples with acetone were subjected to a cold ultra-sound bath during 2 min. Extraction occurred at −20 °C during 24 h in the dark to prevent pigment degradation. After extraction samples were centrifuged at 4000 rpm during 15 min at 4 °C. For pigment analysis it was employed the Gauss-Peak Spectra method [24]. Previous works proved the sensitivity and accuracy of this method by comparison with simultaneous measurements using HPLC producing similar results to this last technique [24]. Samples were scanned in a dual beam spectrophotometer from 350 nm to 750 nm at 0.5 nm steps. The absorbance spectrum was introduced in the GPS fitting library, using SigmaPlot Software. The employment of this library allowed to identify and quantify Chlorophyll a (MgChl a), Chlorophyll b (MgChl b), Zinc-substituted Chlorophyll a (ZnChl a), Zinc-substituted Chlorophyll b (ZnChl b), Pheophytin a (Pheo a), Antheraxanthin (Anthera), β-carotene, Lutein, Violoxanthin (Viola) and Zeaxanthin (Zea). In order to better evaluate the light harvesting and photo-protection mechanisms the De-Epoxidation State (DES) was calculated as:

$$DES = \frac{[Anthera] + [Zea]}{[Viola] + [Anthera] + [zea]}$$

2.5. Anti-oxidant enzyme assays

Enzyme extraction was performed at 4 °C and all the assays at room temperature. Briefly, it was used a proportion of 500 mg of seeds leaves for 8 ml of 50 mM sodium phosphate buffer (pH 7.6) with 0.1 mM Na-EDTA, for extraction. The homogenate was centrifuged at 8923 rpm for 20 min, at 4 °C, and the supernatant was used for the enzymatic assays. Catalase activity was measured according to the method of Teranishi et al. [51], by monitoring the consumption of H_2O_2, and consequent decrease in absorbance at 240 nm. (ε = 39.4 mM^{-1} cm^{-1}). The reaction mixture contained 50 mM of sodium phosphate buffer (pH 7.6), 0.1 mM of Na-EDTA, and 100 mM of H_2O_2. The reaction was started with the addition of the extract. Ascorbate peroxidase was assayed according to Tiryakioglu et al. [53]. The reaction mixture contained 50 mM of sodium phosphate buffer (pH 7.0), 12 mM of H_2O_2, 0.25 mM L-ascorbate. The reaction was initiated with the addition of 100 μL of enzyme extract. The activity was recorded as the decrease in absorbance at 290 nm and the amount of ascorbate oxidized was calculated from the molar extinction coefficient of 2.8 mM^{-1} cm^{-1}. Guaiacol peroxidase was measured by the method of Bergmeyer et al. [3] with a reaction mixture consisting of 50 mM of sodium phosphate buffer (pH 7.0), 2 mM of H_2O_2, and 20 mM of guaiacol. The reaction was initiated with the addition of 100 μL of enzyme extract. The enzymatic activity was measured by monitoring the increase in absorbance at 470 nm (ε = 26.6 mM^{-1} cm^{-1}). Superoxide dismutase

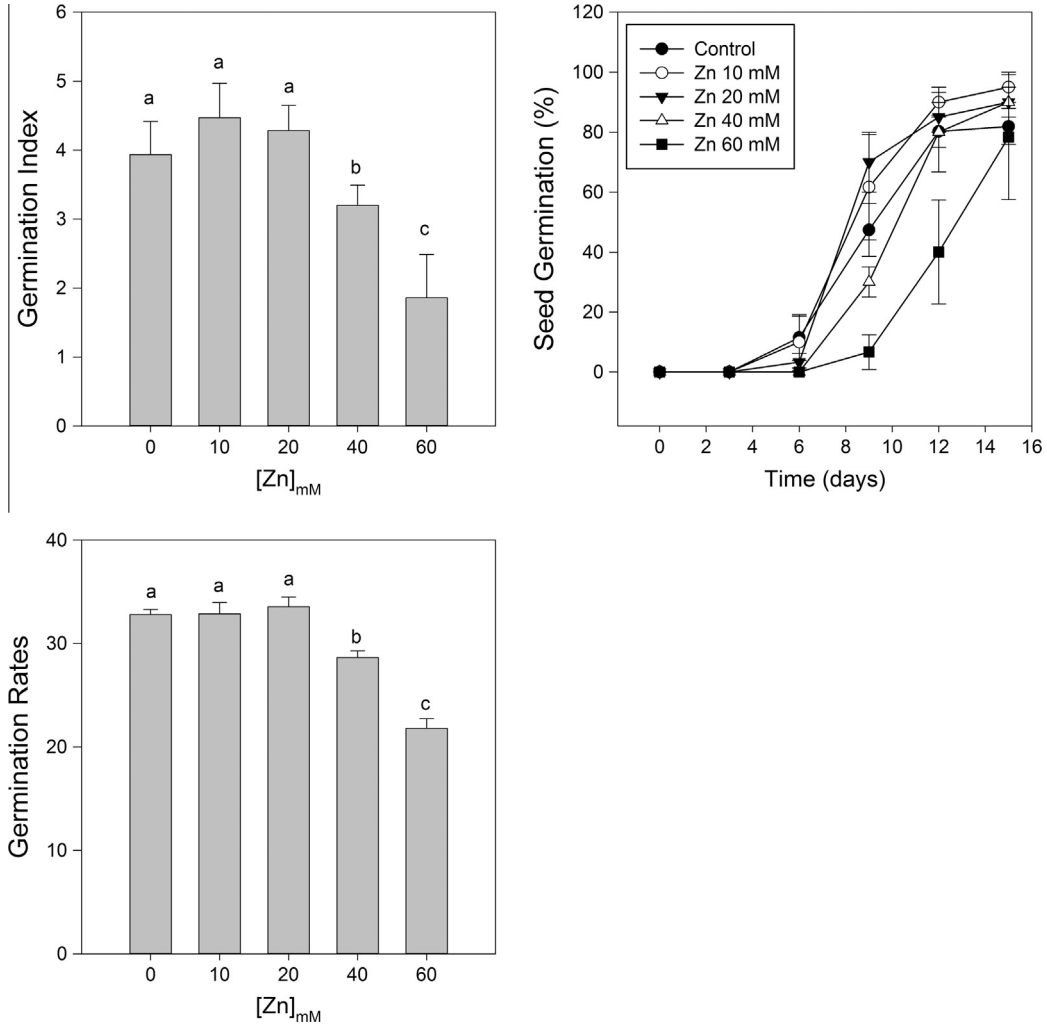

Fig. 1. Seed germination (%), Germination Index and Rates of *J. acutus* exposed to increasing levels of Zn (average ± standard deviation; letter indicate significant ($p < 0.05$) differences among treatments).

activity was assayed according to Marklund and Marklund [28] by monitoring the reduction of pyrogallol at 325 nm. The reaction mixture contained 50 mM of sodium phosphate buffer (pH 7.6), 0.1 mM of Na-EDTA, 3 mM of pyrogallol, Mili-Q water. The reaction was started with the addition of 10 μL of enzyme extract. Control assays were done in the absence of substrate in order to evaluate the auto-oxidation of the substrates.

2.6. Statistical analysis

In order to evaluate the statistical significance between the results obtained among treatments, ANOVA one-way tests were employed using Statistica Software 10 (StataSoft Inc.). Spearman correlations were applied in order to evaluate the existence of direct effects between the metal concentrations and the biological variables.

3. Results

3.1. Seed germination, growth and Zn uptake

Germination percentage was determined in presence of several Zn treatments. Independently of the applied treatment, germination only occurred after 6 days (Fig. 1) with visible increases until day 14. As could be observed, the highest germination percentage was obtained in individuals exposed to 10 mM Zn, reaching almost 100%, being higher than in the control group. At the highest Zn concentration applied (60 mM), seeds suffered a hindrance in germination start. Comparing germination rates between control and 20 mM of Zn treatment, a slightly increase in this parameter was noticed. However, with the application of higher Zn concentrations, germination rates suffered a decrease. This was even more evident when analyzing the Germination Index. Again, a maximum value was detected in individuals exposed to 10 mM of Zn and a strong decrease in individuals subjected to highest Zn concentrations (40 and 60 mM).

The seedling length of plants treated with 10 mM Zn showed almost no signs of disturbance, although the same could not be observed in the remaining treatments (Fig. 2). With increasing exogenous Zn dose, seedlings length showed a marked and significant reduction while compared to the control group. Overlooking to the aboveground biomass, a marked decrease could be observed with increasing Zn doses (Fig. 3).

Zinc content in *J. acutus* seedlings, exposed to increasing levels of metal, showed a significant and proportional increase to the applied dose, being this more evident at the highest Zn concentration (Fig. 4). Individuals exposed to 20 and 40 mM of Zn, showed rather similar values of Zn accumulation in their tissues. Since Zn is an essential element in plant nutrition, it is present in nutrient solution, leading to a basal accumulation even in control seedlings.

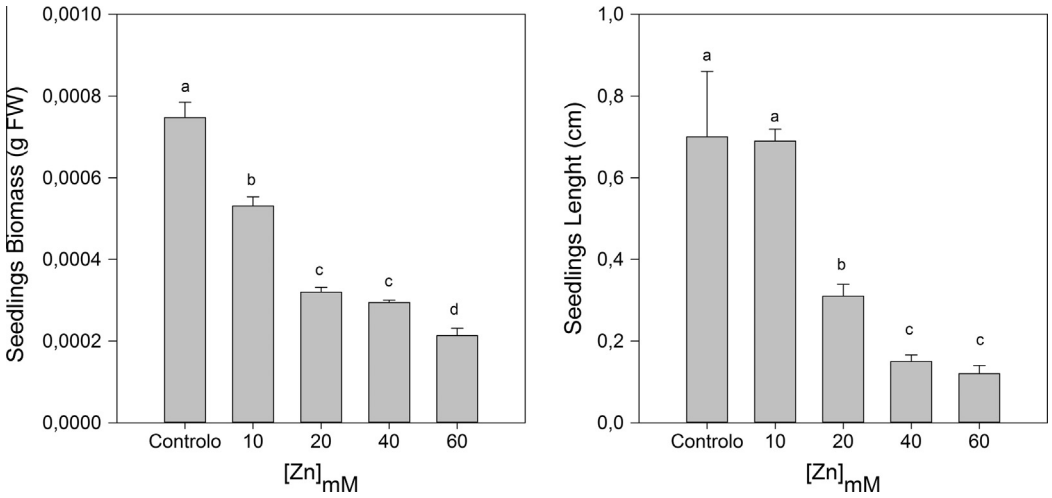

Fig. 2. Seed biomass (g) and length (cm) of *J. acutus* seedlings exposed to increasing levels of Zn (average ± standard deviation; letter indicate significant ($p < 0.05$) differences among treatments).

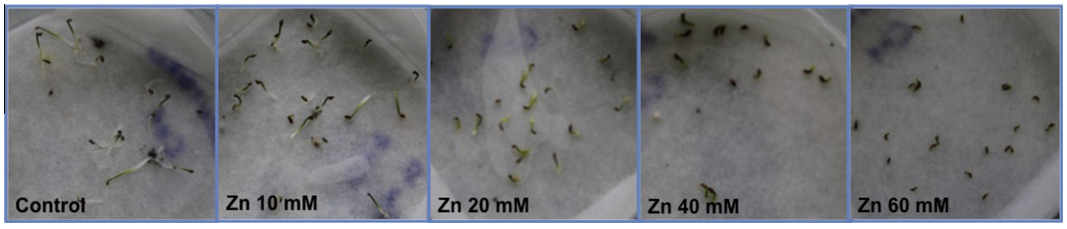

Fig. 3. *J. acutus* seedlings exposed to increasing levels of Zn.

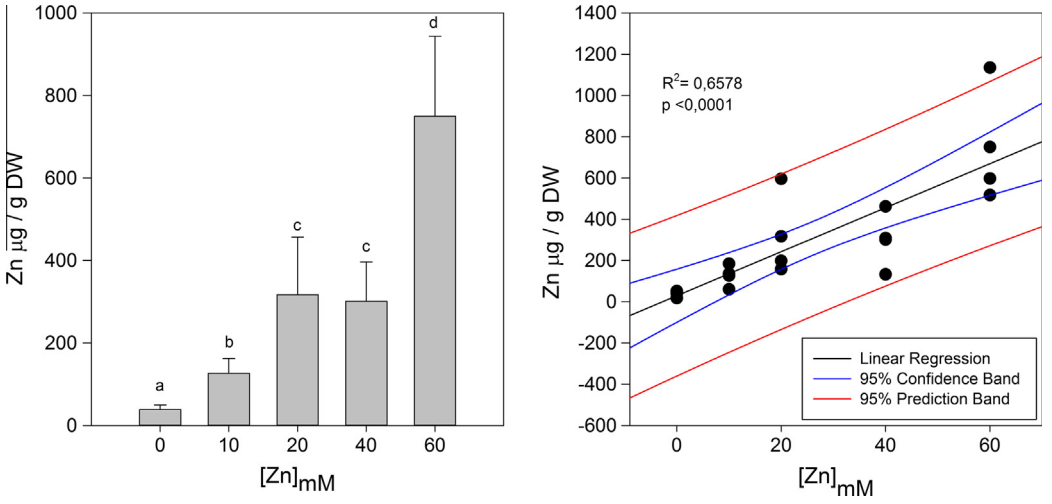

Fig. 4. Seedling Zn content exposed to increasing levels of Zn (average ± standard deviation; letter indicate significant ($p < 0.05$) differences among treatments) and linear regression between Zn treatment and the Zn concentration in the seedlings tissue.

A linear and highly significant correlation could be observed between exogenous and endogenous Zn concentrations, typical from a dose-dependent accumulation.

3.2. Steady state chlorophyll a fluorescence

Regarding maximum and operational PSII quantum efficiencies, a decrease was registered in the presence of Zn, more evident in individuals subjected to higher Zn doses. With increasing Zn concentration, both PSII efficiency parameters declined. However, the lowest value of dark-adapted efficiency (maximum efficiency) was obtained upon the application of 60 mM of Zn, while for the light-adapted efficiency (operational efficiency) this already could be observed at 40 mM of Zn, although with very similar values to the verified in plants treated with 60 mM of Zn. Regarding variable fluorescence, both dark-adapted and light adapted seedlings showed a marked decrease, having its minimum value at the higher Zn dose (60 mM) (see Fig. 5).

Treatments with higher concentrations of Zn (40 and 60 mM) led to a total absence of photosynthetic activity (α) and

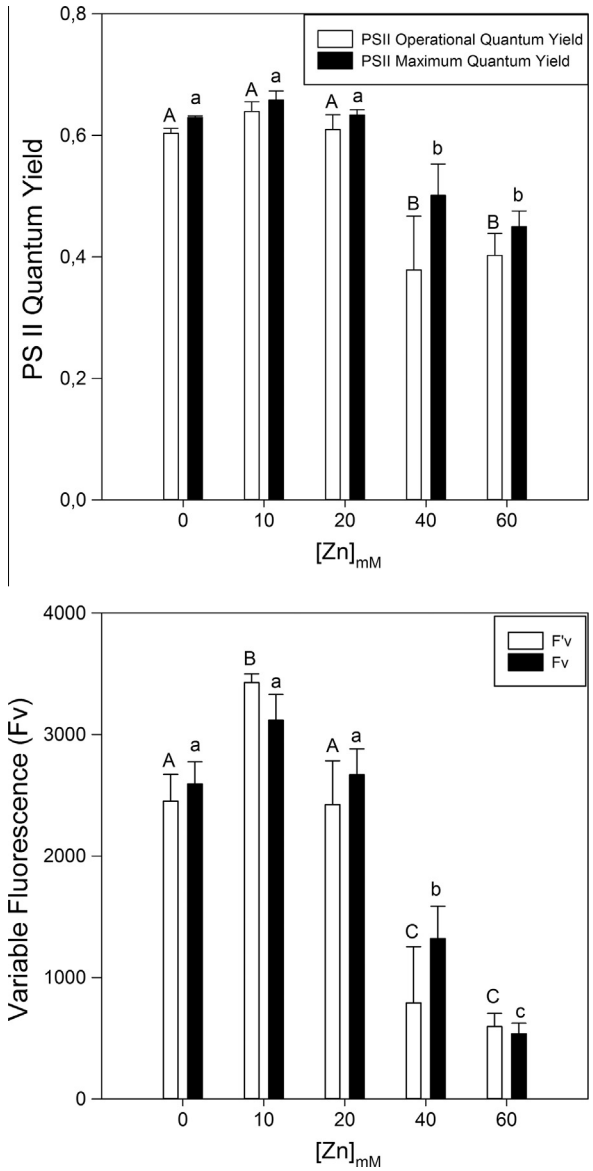

Fig. 5. PSII quantum efficiencies and variable fluorescence *J. acutus* seedlings exposed to increasing levels of Zn (average ± standard deviation; letter indicate significant ($p < 0.05$) differences among treatments).

impairment of the onset of light saturation (E_k), as shown in Fig. 6. These Zn doses also caused a noticeable decline on rETR at different light levels, to the ones verified under photo-inhibition conditions at lower Zn concentrations. Consequently, the maximum rETR also showed a marked decrease in plants exposed to higher Zn doses.

3.3. Kautsky curves and transient OJIP parameters

In this analysis, control and 10 mM Zn treated plants showed an identical fluorescence values in photochemical phase, corresponding to O–J phase. All individuals exposed to higher Zn doses showed a decrease in this phase. The differences between treatments were more evident at the thermal phase (J–I–P), as shown in Fig. 7. The increase in the thermal phase was higher at the 10 mM Zn, being even above the control. On the other hand, the lowest thermal phase was found at the highest zinc treatment. Looking into more detail to the data from OJIP curves, analyzing the driving forces variation, new data arises (Fig. 8). The driving force for photosynthesis (DF_{ABS}) was the most affected parameter with increasing Zn doses. Looking to the partial forces that together compose this last one, it could be observed that this marked decrease was mainly due to a decline in the driving forces derived from trapping of excitation energy ($DF\psi$) and involved in the conversion of excitation energy to electron transport ($DF\varphi$), although at a minor extent. On the other hand, light energy absorption (DF_{RC}) was not affected along the range of tested Zn concentrations, being constant along treatments. Overlooking the grouping probability between the two PSII subunits a clear decoupling between the two units was evident at the highest Zn concentrations.

3.4. Pigment concentrations

Regarding the pigments concentration (Table 2), it is possible to observe a fluctuation of both chlorophyll pigments (MgChl a and b) concentrations along zinc treatments, increasing in plants subjected to 10 and 20 mM of Zn and decreasing in seedlings exposed to higher Zn doses, with MgChl a and b lowest concentrations observed in individuals exposed to 10 mM Zn. Also the chl a/b ratio and the Chlorophyll Degradation Index (CDI) showed a marked decrease with increasing Zn dose, being lower at 40 mM and 60 mM, respectively (Fig. 9).

In relation to carotenoids, violaxanthin was the only xanthophyll that suffered a decrease along with increasing Zn concentrations (Table 2). On the other hand, the remaining carotenoids quantified in this study, showed increases in their concentration along with the crescent zinc gradient, with higher concentrations at 20 mM for Antheraxanthin and β-carotene, 10 mM for Violaxanthin and at 60 mM for Lutein and Zeaxanthin. Concomitantly, the de-epoxidation state, in straight relation to the xanthophyll concentrations, showed a significant decrease with increasing Zn dose, reaching a minimum at 40 mM (Fig. 9). As a result of this carotenoid and chlorophyll dynamics, total carotenoid to total chlorophyll ratio showed a marked increase along the applied Zn doses.

Regarding heavy metal substituted chlorophylls (Fig. 10), ZnChl a showed an increase at 10 mM, contrary to MgChl a. At 20 mM of Zn, both ZnChl a and MgChl a continued to increase, with this last reaching its maximum at this Zn dose. However, at 40 mM both ZnChl a and MgChl a registered a slightly decrease in their concentrations. In individuals exposed to higher Zn dose, both type of chlorophylls concentrations increased again and with ZnChl a attaining its maximum. ZnChl b presented a dose–response pattern with a progressive increase as with the Zn treatment augmentation, reaching a maximum concentration at 60 mM.

3.5. Antioxidant enzymatic activities

Observing the data relative to antioxidant enzymes (Fig. 11), different activity patterns were detected. Regarding CAT, this enzyme only showed detectable activity in individuals subjected to the highest Zn concentration. On the other hand, SOD activity seemed to respond proportionally to increasing concentration of zinc, presenting a maximum activity at 60 mM treatment. GPx activity showed a very similar and significant dose–response pattern to Zn concentrations applied. Although with a more erratic pattern APx activity also points out to a similar trend of increase along the applied Zn gradient.

3.6. Overall Zn metabolic interferences

Overlooking the correlation matrix presented in Table 3 all the above-mentioned results are confirmed to be a consequence of the Zn dose to which seedlings were exposed. Almost all the evaluate parameters present good correlations, not only with the endogenous Zn concentrations but also with the exogenous Zn

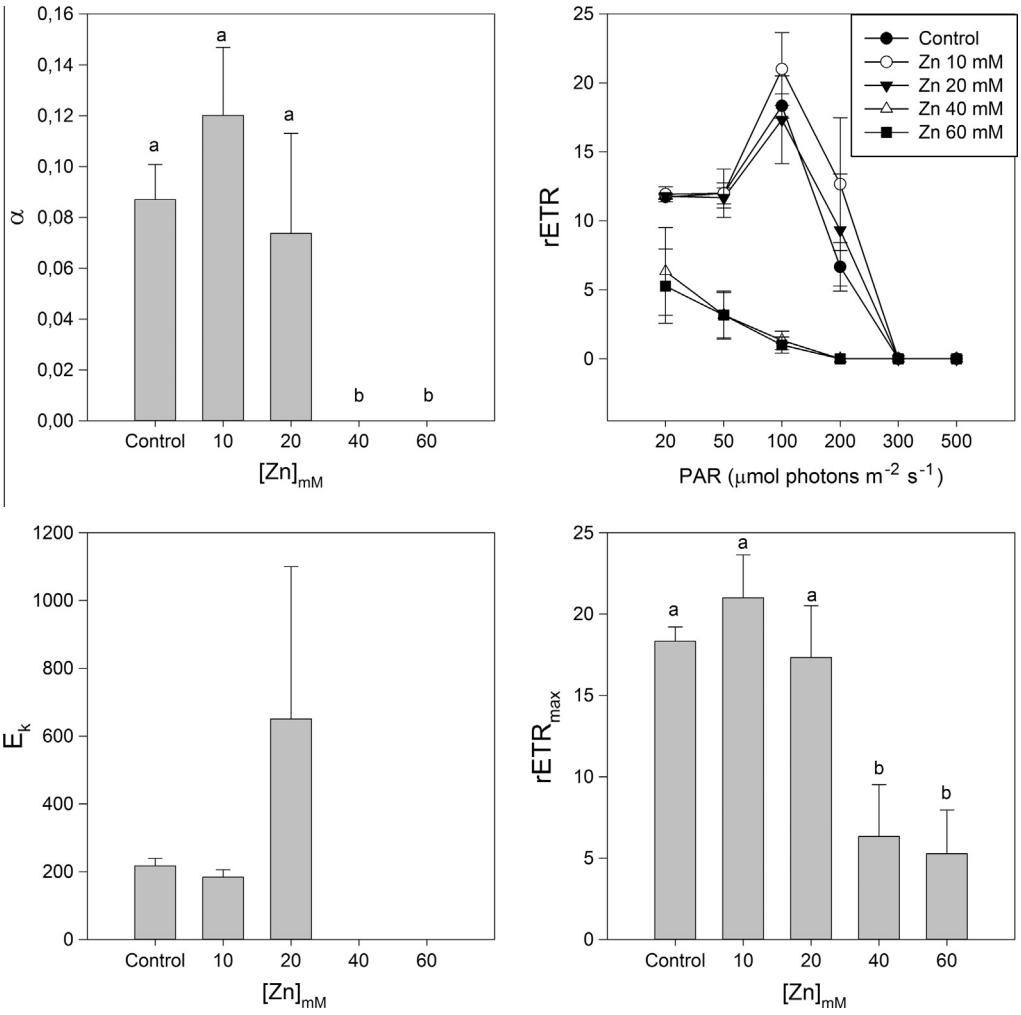

Fig. 6. Photosynthetic efficiency (α), onset of light saturation (E_k) and electron transport rates (ETR) in *J. acutus* seedlings exposed to increasing levels of Zn (average ± standard deviation; letter indicate significant ($p < 0.05$) differences among treatments).

concentration applied. While in most cases Zn application lead to a decrease in the evaluated parameters, anti-oxidant enzymes, Zn-substituted chlorophylls, pheophytin, b-carotene, zeaxanthin and carotenoid to chlorophylls ratio showed an evident positive feedback to Zn application. In sum all counteractive measures proxies showed an enhancement in Zn exposed seedlings while the parameters directly related to the primary production showed negative and significant correlations.

4. Discussion

The bioprospection of plant species that could be used as biotools for managing heavy metal pollution is one of the fundamental guidelines for designing and developing of effective methodologies for environmental remediation. Nevertheless and with equally high importance arises the need to evaluate how potentially hyperaccumulator species behave and tolerate acute metal stress and more importantly how it impacts their primary productivity. From this point of view *J. acutus* arises as possible biomonitor and hyperaccumulator specie, tolerating exogenous Zn concentrations as high as 60 mM. In the presence of intermediate and higher Zn concentrations, tissues from seedlings presented internal values of Zn above the upper toxic levels for higher plants, which are considered to be 100–500 μg g^{-1} [21]. At this level, this specie showed

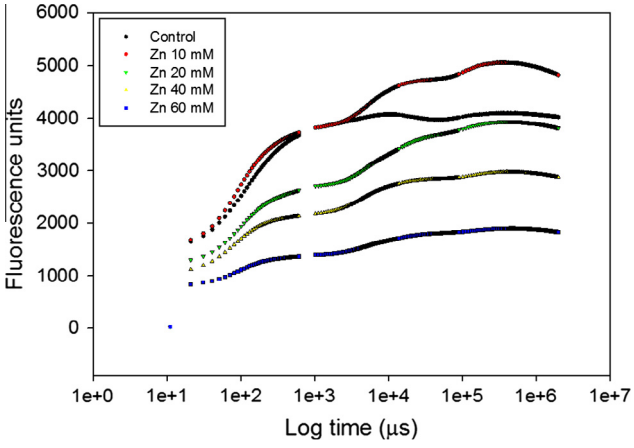

Fig. 7. Transient light curves (OJIP curves) in *J. acutus* seedlings exposed to increasing levels of Zn (average values).

a very high tolerance to Zn, with only 6% depletion in the number of germinated seeds at the highest Zn tested dose. Considering the definition of EC_{50} as the substrate Zn concentration resulting in 50% biomass reduction [41] this elevated tolerance and uptake

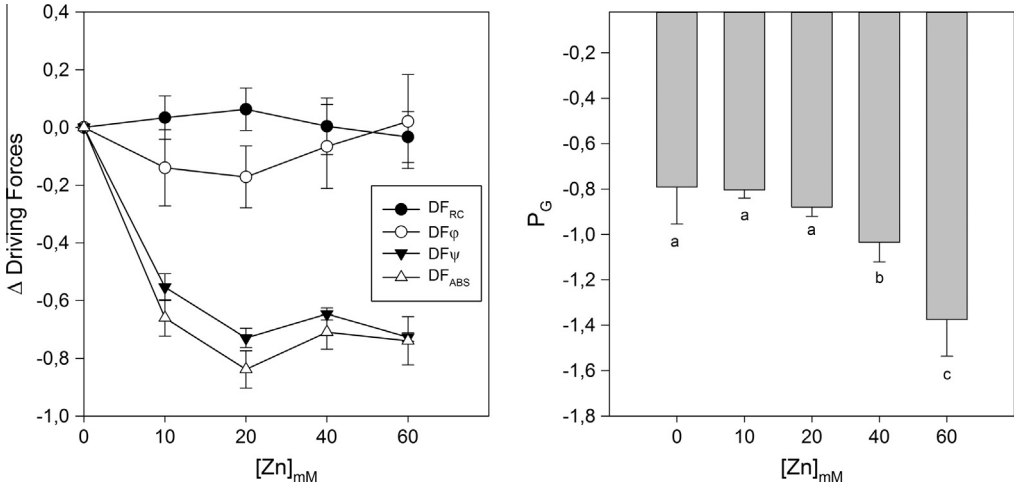

Fig. 8. OJIP curves derived driving forces and grouping probability (P_G) in *J. acutus* seedlings exposed to increasing levels of Zn (average ± standard deviation; letter indicate significant ($p < 0.05$) differences among treatments).

Table 2
Chlorophyll and degradation products and carotenoid concentration in *J. acutus* seedlings exposed to increasing levels of Zn (average ± standard deviation; letter indicate significant ($p < 0.05$) differences among treatments).

Zn (mM)	MgChl a	MgChl b	Pheo a	Anther	β-Carot	Lutein	Viola	Zea
0	339.8 ± 38.4^{a}	129.1 ± 15.4	8.8 ± 2.1^{a}	7.0E-08 ± 7.0E-08^{a}	11.2 ± 1.47^{a}	24.6 ± 2.3^{a}	24.9 ± 2.1	11.9 ± 1.6^{a}
10	188.9 ± 5.6	123.9 ± 5.3	107.4 ± 4.9^{b}	17.9 ± 5.4	34.5 ± 4.7^{b}	21.3 ± 4.3^{a}	11.2 ± 2.8	47.2 ± 9.5
20	274.9 ± 19.7^{b}	180.8 ± 22.5	187.9 ± 8.9^{c}	31.6 ± 4.4^{b}	66.9 ± 7.6^{c}	40.6 ± 4.7^{b}	8.2 ± 1.9	72.8 ± 8.1^{b}
40	208.9 ± 18.3	168.8 ± 7.6	171.1 ± 14.2^{c}	21.2 ± 10.1	53.1 ± 5.4^{c}	28.4 ± 10.2^{a}	7.5 ± 7.5	63.9 ± 11.5^{b}
60	247.6 ± 16.1^{b}	150.5 ± 7.1	226.7 ± 16.5^{d}	31.3 ± 5.1^{b}	66.8 ± 1.1^{c}	45.8 ± 2.6^{b}	8.4 ± 4.4	73.7 ± 0.9^{b}

becomes even more evident. Even at the highest Zn concentration, the growth inhibition only accounts to approximately 30% of control seedlings biomass, being remarkably higher than for other plants germinated at higher Zn tested concentration [41]. Considering the results here presented, the EC_{50} value for Zn in *J. acutus* is in the range of 10–20 mM of this metal. For other plant species, this inhibition value was found to be within the range of 1.2–3.4 mM [41,40]. In previous works, *Juncus effusus* showed a more pronounced growth inhibition at much lower Zn concentrations (0.7 mM; [33]. Despite this growth inhibition, it was also verified a very good dose–response relationship between exogenous and plant tissue Zn concentrations, being an excellent evidence of a phytoremediator ability and of a biomonitor potential under acute toxicity. Metal hypertolerance in plants has been described as an ecophysiological adaptation to metalliferous environments [17], thus the metabolic performance of Zn-affected seedlings was also investigated. Although net photosynthesis depends on the carbon sequestration efficiency, the light harvesting mechanisms also influences it. This last one has proved to be very sensitive to abiotic stresses, in particular in halophytes, showing rapid feedbacks to any disturbance that affect the PSII apparatus [15,13,14]. Variable fluorescence, a well know proxy of abiotic stress [15,12], as well as PSII maximum and operational quantum yields showed significant decreases, being this also a well-known proxy of photo-inhibition processes [34]. Monnet et al. [35] found that antennae pigments destruction due to excessive heavy metal accumulation may disturb maximum PSII photochemistry. This decrease in PSII quantum yields was mostly due to a decrease in basal fluorescence, F_0 affecting negatively the F_v/F_0 ratio (data not shown). This decrease in F_v/F_0 ratio, was previously reported in *D. sanguinea*, as being a reflection of changes in thylakoid structure on PSII electron donor sites [47]. This reduction suggests a change in thylakoids membrane structure, inevitably affecting electron transport, and/or leading to the destruction of chlorophyll pigments [54]. Heavy metals are known to block PSII electron transport [23]. The PSII is preferentially bound with divalent cations as Zn and Mn [55]. Moreover this possible higher affinity for Zn, the substitution of Mn by this metal at the site of water photolysis, inhibits oxygen production and electron transfer [44]. This substitution is possible due to the electronic similarities of these two ions [54]. In fact, electron transport rate was severely affected by Zn in seedlings exposed to higher concentrations of this metal leading to a decrease in their maximum electronic transport rate, presenting lower light saturation and consequently lower photosynthetic light harvesting efficiencies. Looking deeper into the light harvesting processes and into the energy flux transports, Zn effects on steady-state fluorescence are clarified. Although light absorption capacity was not affected by Zn exposure and uptake, the entrapment of this energy flux into the photosynthetic apparatus and transport throughout the electronic chain was severely impaired. On the basis of this inefficiency are probably the non-functional Zn-chlorophylls. Prasad et al. [43] suggested that the substitution of Mg by Zn might also damage the chlorophyll synthesis system, leading to the accumulation of chlorophyll degradation products like, pheophytins. Recently Küpper et al. [24] developed a method that allows to accurately determining Zn-substituted chlorophylls concentrations. Overlooking the data obtained throughout this technique, all above-mentioned results are confirmed. There is a strong linear correlation between both Zn concentration applied exogenously and the tissue Zn concentration with the concentration of both ZnChl a and b. This substitution also leads to a decrease in the functional Mg-chlorophyll concentration, by Mg substitution by Zn. Simultaneously an increase in MgChl b could also be detected, concomitant with the decrease in chl a/b ratio and indicative of a stress conditions as was previously found in other halophytes under ionic stress [12]. Due to its lack of

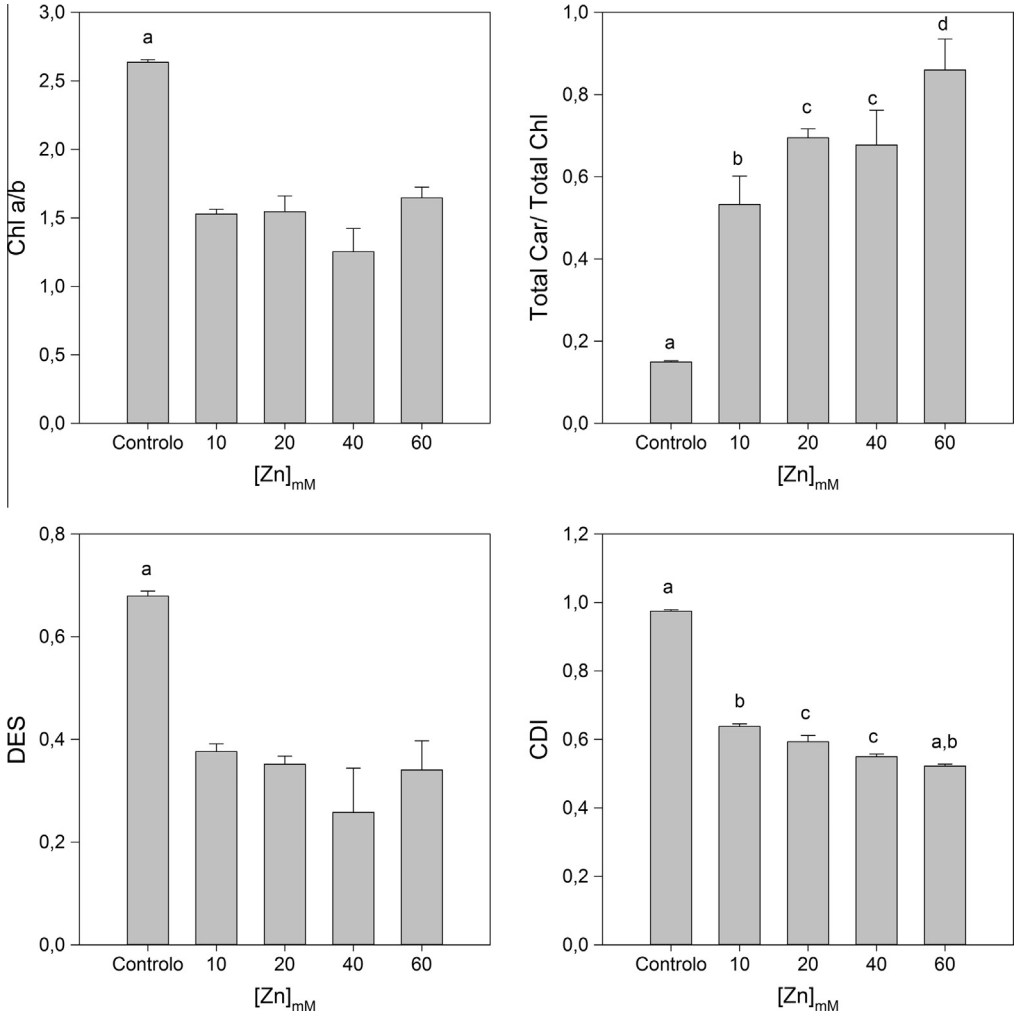

Fig. 9. Pigment ratios and indices in *J. acutus* seedlings exposed to increasing levels of Zn (average ± standard deviation; letter indicate significant ($p < 0.05$) differences among treatments).

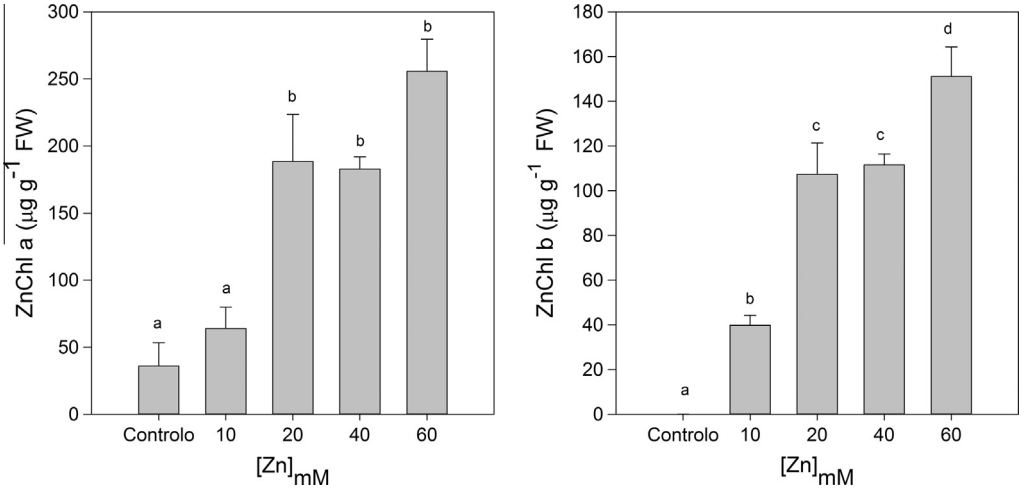

Fig. 10. ZnChl a and b in *J. acutus* seedlings exposed to increasing levels of Zn (average ± standard deviation; letter indicate significant ($p < 0.05$) differences among treatments).

efficiency for light harvesting processes (decrease in the trapping of excitation energy, DFψ), the seedlings photosynthetic efficiency (α) and maximum ETR were significantly depleted (decrease in ETRmax and in the conversion of excitation energy to electron transport, DFφ). All these impairments lead to an inevitable accumulation of redox energy inside the cells [10]. Also, PSII sensitivity

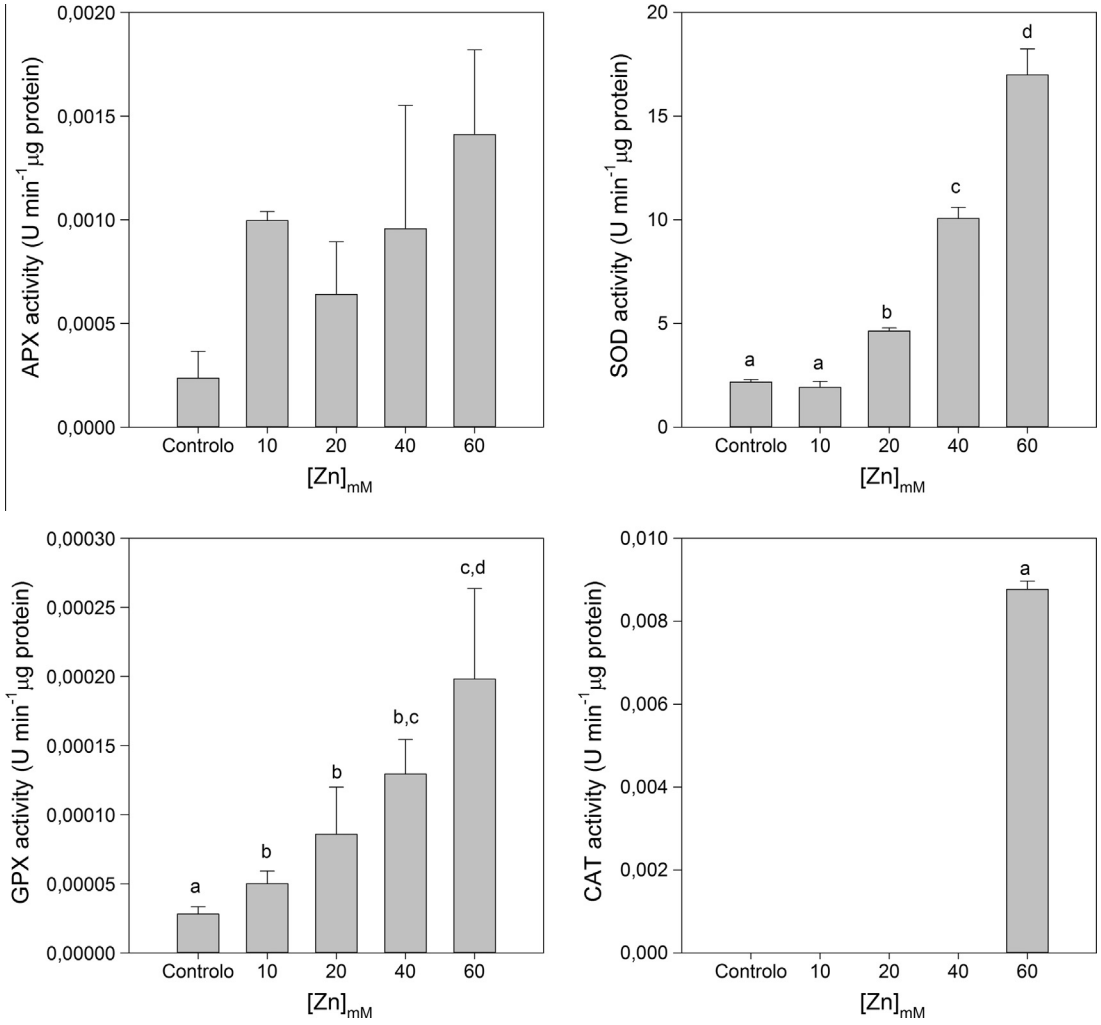

Fig. 11. Catalase, ascorbate and guaiacol peroxidase and superoxide dismutase activities in *J. acutus* seedlings exposed to increasing levels of Zn (average ± standard deviation; letter indicate significant ($p < 0.05$) differences among treatments).

in seedlings under high Zn concentrations could be related to interactions between Zn and the PSII reaction center. Besides this Mg-substitution in the chlorophyll molecule, due to the similarities in ion radius of bivalent cations (Mn, Fe, Mg and Zn), excess Zn can shift certain physiological equilibriums by local competition at various binding sites [35]. Zinc can strongly affect the photochemical reactions of photosystems, for e.g. by displacement of non-heme Fe^{2+} in the PSII [19]. Monnet et al. [35] showed that the substitution of Mn^{2+} by Zn^{2+} also alters the oxygen-evolving complex activity. Not only electron transport is processed at lower rates in Zn-stressed plants, but also the size of quinone pools (directly proportional to the area above the Kautsky curve) is severely reduced at the PSII acceptor side [50,20]. The OJIP-test also provided means to calculate the overall P_G or connectivity between PSII antennae. This parameter accounts for all energetic communication pathways between neighbor PSII antennae [49,39]. There is gradual loss of connectivity between PSII antennae units, being more evident at the highest Zn concentrations, directly related to lacks of energetic connectivity between the two PSII subunits and therefore impairing energetic transport [49]. Nevertheless, seedlings still acquire enough light energy for photosynthetic biomass production even under elevated Zn concentrations. Nevertheless, this leads to an accumulation of excessive redox potential inside the cells with inevitable formation of reactive oxygen species (ROS) that could endanger all cellular mechanisms. Here resides the secret behind Zn hyperaccumulation and tolerance in *J. acutus* under acute toxicity. Both chronic and acute exposures to heavy metals are known to induce rather efficient anti-oxidant pathways in halophytes [12,15]. *Juncus acutus* is no exception. Excluding catalase, that appears to be an ultimate defence system playing a significant role only at extremely high Zn concentrations, all remaining anti-oxidant enzymatic activities showed a proportional response toexogenous and *in vivo* Zn concentrations. Not only Zn, like other heavy metals, generate ROS by interaction with several molecules and cellular components, but also all the redox potential accumulated due to ETC impairment acts as generator of these damaging molecules. Seedlings appear to be very well prepared with highly efficient enzymatic machinery, counteracting ROS generation and responding proportionally to the applied Zn dose. This efficient defence system is on the basis of cellular redox homeostasis allowing all photochemical processes to occur, even though at slower rates due to direct interference from Zn with PSII and more importantly with active center of the chlorophyll molecule.

5. Conclusions

Bioprospection of potential heavy metal hyperaccumulators focuses not only the phytoremediative ability of the specie towards

Table 3
Correlation coefficients (r^2) between the analyzed parameters and the verified Zn concentrations in the seedlings tissues (mg g DW^{-1}) and the applied exogenous Zn concentration ($^{*}p < 0.05$; $^{**}p < 0.01$; $^{***}p < 0.001$).

Parameter	Zn (μg g DW^{-1})	Exogenous Zn (mM)
Germination index	−0.76***	−0.83***
Germination rate	−0.75**	−0.89***
Seedling biomass	−0.72**	−0.87***
Seedling length	−0.67**	−0.86***
Biomass/length ratio	−0.40	−0.72**
F'_v	−0.49	−0.82***
PSII operational quantum yield	−0.46	−0.76***
F_v	−0.64*	−0.89***
PSII maximum quantum yield	−0.53*	−0.85***
Photosynthtic efficiency (a)	−0.42	−0.75**
Maximum ETR	−0.54*	−0.80***
Onset light saturation (E_k)	−0.26	−0.31
DF_{RC}	0.05	−0.17
DFφ	−0.03	0.15
DFψ	−0.59*	−0.69**
DF_{ABS}	−0.52*	−0.58*
P_G	−0.63**	−0.78***
MgChl a	0.01	−0.32
MgChl b	0.39	0.34
Pheo A	0.77***	0.84***
Antheraxanthin	0.55*	0.58*
β Carotene	0.72**	0.74**
Violaxanthin	−0.38	−0.50
Zeaxanthin	0.66**	0.69**
De-epoxidation state (DES)	−0.43	−0.62*
Chl a/b ratio	−0.29	−0.54*
Total car/total Chl	0.63*	0.81***
Chl degradation index	−0.56*	−0.77***
ZnChl a	0.82***	0.86***
ZnChl b	0.83***	0.90***
CAT activity	0.74**	0.79***
APx activity	0.28	0.52*
GPx activity	0.58*	0.77***
SOD activity	0.80***	0.97***

a specific metal while producing high amounts of biomass, but should also focus in the health status of the plant as well as possible causes and counter-measures of stress. This last approach can also provide to be a source of important biomarkers of acute toxicity for biomonitoring proposes. *Juncus acutus* appears as a potential Zn-hyperaccumulator as well as potential model specie for studying Zn accumulation under severe toxicity and its biochemical implications. Not only this specie appears to be highly tolerant to high Zn concentrations, but it can also overcome efficiently the damage produced during this uptake by proficiently dissipating excessive cellular redox potential accumulated, driven essentially by Zn incorporation into the chlorophyll molecule. Thus, this specie should be considered in further studies as a potential phytoremediator for both terrestrial and aquatic areas. Also the here presented biochemical and biophysical test battery appears to provide efficient biomarkers of Zn acute toxicity as powerful tools for biomonitoring in metalliferous environments.

Acknowledgments

The authors would like to thank to the "Fundação para a Ciência e Tecnologia (FCT)" for funding the research in the Centre of Oceanography (CO) throughout the project PEst-OE/MAR/UI0199/2011 and this specific work throughout the ECOSAM project (PTDC/AAC-CLI/104085/2008). B. Duarte investigation was supported by FCT throughout a PhD Grant (SFRH/BD/75951/2011).

References

[1] S. Beer, M. Ilan, A. Eshel, A. Weil, I. Brickner, The use of pulse amplitude modulated (PAM) fluorometry for in situ measurements of photosynthesis in two Red Sea Faviid corals, Mar. Biol. 131 (1998) 607–612.
[2] S. Beer, B. Vilenkin, A. Weil, M. Veste, L. Susel, A. Eshel, Measuring photosynthesis in seagrasses by pulse amplitude modulated (PAM) fluorometry, Mar. Ecol. Prog. Ser. 174 (1998) 293–300.
[3] H.U. Bergmeyer, K. Gawehn, M. Grassl, Enzymes as biochemical reagents, in: H.U. Bergmeyer (Ed.), Methods in Enzymatic Analysis, Academic press, New York, 1974.
[4] I. Caçador, J.M. Neto, B. Duarte, D.V. Barroso, M. Pinto, J.C. Marques, Development of an Angiosperm Quality Assessment Index (AQuA – Index) for ecological quality evaluation of Portuguese water bodies – a multi-metric approach, Ecol. Ind. 25 (2013) 141–148.
[5] I. Caçador, C. Vale, F. Catarino, The influence of plants on concentration and fractionation of Zn, Pb, and Cu in salt marsh sediments (Tagus Estuary, Portugal), J. Aquat. Ecosyt. Health 5 (1996) 193–198.
[6] J. Cambrollé, J.M. Mancilla-Leytón, S. Muñoz-Vallés, T. Luque, M.E. Figueroa, Zinc tolerance and accumulation in the salt-marsh shrub *Halimione portulacoides*, Chemosphere 86 (2012) 867–874.
[7] H.B. Chang, C.W. Lin, H.J. Huang, Zinc-induced cell death in rice (*Oryza sativa* L.) roots, Plant Growth Regul. 46 (2005) 261–266.
[8] A. Cuypers, K. Smeets, J. vangronsveld, Heavy metal stress in plants, in: H Hirt (Ed.), Plant Stress Biology, WILEY-VCH Verlag GmbH & Co., KGaA, Weinheim, 2009, pp. 161–178.
[9] A. Cuypers, J. Vangronsveld, H. Clijsters, The redox status of plant cells (AsA and GSH) is sensitive to zinc imposed oxidative stress in roots and primary leaves of *Phaseolus vulgaris*, Plant Physiol. Biochem. 39 (2001) 657–664.
[10] D. De Magalhaes, C.P. Cardoso, R.M. Dos Santos, Physiological and photosynthetic responses of *Synechocystis aquatilis f. aquatilis* (Cyanophyceae) to elevated levels of zinc, J. Phycol. 40 (2004) 496–504.
[11] B. Duarte, I. Caçador, J.C. Marques, I. Croudace, Tagus Estuary salt marshes feedback to sea level rise over a 40-year period: insights from the application of geochemical indices, Ecol. Ind. 34 (2013) 268–276.
[12] B. Duarte, D. Santos, I. Caçador, Halophyte anti-oxidant feedback seasonality in two salt marshes with different degrees of metal contamination: search for an efficient biomarker, Funct. Plant Biol. 40 (2013) 922–930.
[13] B. Duarte, D. Santos, J.C. Marques, I. Caçador, Ecophysiological adaptations of two halophytes to salt stress: photosynthesis, PS II photochemistry and anti-oxidant feedback – implications for resilience in climate change, Plant Physiol. Biochem. 67 (2013) 178–188.
[14] B. Duarte, D. Santos, J.C. Marques, I. Caçador, Biophysical probing of *Spartina maritima* Photo-system II changes during increased submersion periods: possible adaptation to sea level rise, Plant Physiol. Biochem. 77 (2014) 122–132.
[15] B. Duarte, V. Silva, I. Caçador, Hexavalent chromium reduction, uptake and oxidative biomarkers in *Halimione portulacoides*, Ecotoxicol. Environ. Saf. 83 (2012) 1–7.
[16] S.D. Ebbs, L.V. Kochian, Toxicity of zinc and copper to *Brassica* species: implications for phytoremediation, J. Environ. Qual. 26 (1997) 776–781.
[17] M.W. Evangelou, H. Daghan, A. Schaeffer, The influence of humic acids on the phytoextraction of cadmium from soil, Chemosphere 57 (2004) 207–213.
[18] B. Genty, J.-M. Briantais, N.R. Baker, The relationship between the quantum yield of photosynthetic electron transport and quenching of chlorophyll fluorescence, Biochim. Biophys. Acta 990 (1989) 87–92.
[19] C. Jegerschöld, F. MacMillan, W. Lubitz, A.W. Rutherford, Effects of copper and zinc ions on photosystem II studied by EPR spectroscopy, Biochemistry 38 (1999) 12439–12445.
[20] P. Joliot, A. Joliot, Cyclic electron transport in plant leaf, PNAS 99 (2002) 10209–10214.
[21] A. Kabata-Pendias, H. Pendias, Trace Elements in Soils and Plants, CRC Press, Boca Raton, FL, 2001.
[22] H. Kalaji, Govindjee, K. Bosa, J. Koscielniak, K. Zuk-Golaszewska, Effects of salt stress on photosystem II efficiency and CO_2 assimilation of two Syrian barley landraces, Environ. Exp. Bot. 73 (2011) 64–72.
[23] Z. Krupa, M. Baranowka, D. Orzol, Can anthocyanins be considered as heavy metal indicator in higher plant?, Acta Physiol Plant. 18 (1996) 147–151.
[24] H. Küpper, S. Seibert, P. Aravind, A fast, sensitive and inexpensive alternative to analytical pigment HPLC: quantification of chlorophylls and carotenoids in crude extracts by fitting with Gauss-Peak-Spectra, Anal. Chem. 79 (2007) 7611–7627.
[25] H. Küpper, I. Šetlík, M. Spiller, F.C. Küpper, O. Prášil, Heavy metal-induced inhibition of photosynthesis: targets of in vivo heavy metal chlorophyll formation, J. Phycol. 38 (2002) 429–441.
[26] G. Lingua, C. Franchin, V. Todeschini, S. Castiglione, S. Biondi, B. Burlando, V. Parravicini, P. Torrigiani, G. Berta, Arbuscular mycorrhizal fungi differentially affect the response to high zinc concentrations of two registered poplar clones, Environ. Pollut. 153 (2008) 137–147.
[27] K.V. Madhava Rao, T.V.S. Sresty, Antioxidative parameters in the seedlings of pigeonpea (*Cajanus cajan* (L) Millspaugh) in response to Zn and Ni stresses, Plant Sci. 157 (2000) 113–128.
[28] S. Marklund, G. Marklund, Involvement of superoxide anion radical in the autoxidation of pyrogallol and a convenient assay for superoxide dismutase, Eur. J. Biochem. 47 (1974) 464–469.
[29] H. Marschner, Mineral Nutrition in Higher Plants, 2nd ed., Academic Press Limited, London, 1995.
[30] H.J. Marshall, R.J. Geider, K.J. Flynn, A mechanistic model of photoinhibition, New Phytol. 145 (2000) 347–359.
[31] J.J. Martínez-Sánchez, E. Conesa, M.J. Vicente, A. Jiménez, J.A. Franco, Germination responses of *Juncus acutus* (Juncaeae) and *Schoenus nigricans* (Cyperaceae) to light and temperature, J. Arid Environ. 66 (2006) 187–191.

[32] E. Mateos-naranjo, E.M. Castellanos, A. Perez-Martin, Zinc tolerance and accumulation in the halophytic species *Juncus acutus*, Environ. Exp. Bot. 100 (2014) 114–121.
[33] D.J. Matthews, B.M. Moran, M.L. Otte, Screening the wetland plant species *Alisma plantago-aquatica*, *Carex rostrata* and *Phalaris arundinacea* for innate tolerance to zinc and comparison with *Eriophorum angustifolium* and *Festuca rubra* Merlin, Environ. Pollut. 134 (2005) 343–351.
[34] K. Maxwell, G.N. Johnson, Chorophyll fluorescence – a practical guide, J. Exp. Bot. 51 (2000) 659–668.
[35] F. Monnet, N. Vaillant, P. Vernay, A. Coudret, H. Sallanon, A. Hitmi, Relationship between PSII activity, CO_2 fixation, and Zn, Mn and Mg contents of *Lolium perenne* under zinc stress, J. Plant Physiol. 158 (2001) 1137–1144.
[36] E. Mrozek, N. Funicelli, Effect of zinc and lead on germination of *Spartina alterniflora* Loisel seeds at various salinities, Environ. Exp. Bot. 22 (1982) 23–32.
[37] T. Ngo, Y. Zhao, Formation of zinc-chlorophyll-derivative complexes in thermally processed green pears (*Pyrus communis* L.), J. Food Sci. 77 (2007) 397–404.
[38] M.L. Otte, S.J. Bestbroer, J.M. van der Linden, J. Rozema, R.A. Broekman, A survey of zinc, copper and cadmium concentrations in salt marshes plants along the Dutch coast, Environ. Pollut. 72 (1991) 175–189.
[39] D. Panda, D.N. Rao, S.G. Sharma, R.J. Strasser, R.K. Sarkar, Submergence effects on rice genotypes during seedling stage: probing of submergence driven changes of photosystem 2 by chlorophyll a fluorescence induction O–J–I–P transients, Photosynthetica 44 (2006) 69–75.
[40] M.W. Paschke, L.G. Perry, E.F. Redente, Zinc toxicity thresholds for reclamation forb species, Water Air Soil Pollut. 170 (2006) 317–330.
[41] M.W. Paschke, E.F. Redente, D.B. Levy, Zinc toxicity thresholds for important reclamation grass species of the western United States, Environ. Toxicol. Chem. 19 (2000) 2751–2756.
[42] T. Platt, C.L. Gallegos, W.G. Harrison, Photoinhibition of photosynthesis in natural assemblages of marine phytoplankton, J. Mar. Res. 38 (1980) 687–701.
[43] K.V.S.K. Prasad, P. Paradha Saradhi, P. Sharmila, Concerted action of antioxidant enzymes and curtailed growth under zinc toxicity in *Brassica juncea*, Environ. Exp. Bot. 42 (1999) 1–10.
[44] P.J. Ralph, M.D. Burchett, Photosynthesis response of *Halophila ovalis* to heavy metal stress, Environ. Pollut. 103 (1998) 91–101.
[45] G.R. Rout, P. Das, Effect of metal toxicity on plant growth and metabolism: I. Zinc, Agronomie 23 (2003) 3–11.
[46] J.W. Runcie, M.J. Durako, Among-shoot variability and leaf-specific absorbance characteristics affect diel estimates of in situ electron transport of *Posidonia australis*, Aquat. Bot. 80 (2004) 209–220.
[47] E. Skorzynska-Polit, T. Baszynski, Differences in sensitivity of the photosynthetic apparatus in Cd-stressed runner bean plants in relation to their age, Plant Sci. 128 (1997) 11–21.
[48] Z. Stoyanova, S. Doncheva, The effect of zinc supply and succinate treatment on plant growth and mineral uptake in pea plant, Brazil. J. Plant Physiol. 14 (2002) 111–116.
[49] R.J. Strasser, A.D. Stirbet, Estimation of the energetic connectivity of PS II centres in plants using the fluorescence rise O–J–I–P. Fitting of experimental data to three different PS II models, Math. Comput. Simul. 56 (2001) 451–461.
[50] R.J. Strasser, A. Srivastava, Govindjee, Polyphasic chlorophyll a fluorescence transient in plants and cyanobacteria, Photochem. Photobiol. 61 (1995) 32–42.
[51] Y. Teranishi, A. Tanaka, M. Osumi, S. Fukui, Catalase activities of hydrocarbon-utilizing Candida yeast, Agric. Biol. Chem. 38 (1974) 1213–1220.
[52] R.K. Tewari, P. Kumar, P.N. Sharma, Morphology and physiology of zinc-stressed mulberry plants, J. Plant Nutr. Soil Sci. 171 (2008) 286–294.
[53] M. Tiryakioglu, S. Eker, F. Ozkutlu, S. Husted, I. Cakmak, Antioxidant defense system and cadmium uptake in barley genotypes differing in cadmium tolerance, J. Trace Elem. Med Biol. 20 (2006) 181–189.
[54] N. Vaillant, F. Monnet, A. Hitmi, H. Sallanon, A. Coudret, Comparative study of responses in four datura species to zinc stress, Chemosphere 59 (2005) 1005–1013.
[55] F.V. Van Assche, H. Clijsters, Inhibition of photosynthesis by treatment of *Phaseolus vulgaris* with toxic concentration of zinc: effects on electron transport and photophosphorylation, Physiol. Plant. 66 (1986) 717–721.
[56] M. Wójcik, E. Skórzynska-Poli, A. Tukiendorf, Organic acids accumulation and antioxidant enzyme activities in *Thlaspi caerulescens* under Zn and Cd stress, Plant Growth Regul. 48 (2006) 145–155.
[57] X.G. Zhu, Govindjee, N.R. Baker, E.D. Sturler, D.R. Ort, S.P. Long, Chlorophyll a fluorescence induction kinetics in leaves predicted from a model describing each discrete step of excitation energy and electron transfer associated with Photosystem II, Planta 223 (2005) 114–133.